

## New developments in FLUKA

**F. Cerutti<sup>1</sup>, R. Engel<sup>2</sup>, A. Fedynitch<sup>1</sup>, A. Ferrari<sup>1</sup>, A. Mairani<sup>3</sup>, A. Mereghetti<sup>1</sup>,  
S. Roesler<sup>1</sup>, P.R. Sala<sup>4</sup>, P. Schoofs<sup>1</sup>, G. Smirnov<sup>1</sup>, V. Vlachoudis<sup>1</sup>**

<sup>1</sup>CERN, European Laboratory for Particle Physics, Switzerland

<sup>2</sup>KIT, Institut für Kernphysik, Karlsruhe Institute of Technology, Germany

<sup>3</sup>Unità di Fisica Medica, Fondazione CNAO, Italy

<sup>4</sup>INFN, Italy

### Abstract

The FLUKA Monte Carlo code is extensively used at CERN for all beam-machine interactions, radioprotection calculations and facility design for forthcoming projects. Such needs require the code to be consistently reliable over the entire energy range (from MeV to TeV) for all projectiles (the full suite of elementary particles and heavy ions). Outside CERN, among various applications worldwide, FLUKA serves as a core tool for the HIT and CNAO hadrontherapy facilities in Europe. Medical applications further impose stringent requirements in terms of reliability and predictive power, which demands constant refinement of nuclear models and continuous code improvement. This paper presents the latest developments implemented in FLUKA.

### Introduction

FLUKA [1,2] is a general purpose tool for calculations of particle transport and interactions with matter, covering an extensive range of applications spanning from proton and electron accelerator shielding to target design, calorimetry, activation, dosimetry, detector design, accelerator-driven systems, cosmic rays, neutrino physics and radiotherapy. Sixty different particles plus heavy ions can be transported by the code. The energy range covered for hadron-hadron and hadron-nucleus interaction is from threshold up to 10000 TeV, while electromagnetic and  $\mu$  interactions can be dealt with from 1 keV (100 eV for photons) up to 10000 TeV. Nucleus-nucleus interactions are also supported up to 10000 TeV/n. Neutron transport and interactions below 20 MeV down to thermal energies are treated in the framework of a multi-group approach, with cross-section data sets developed for FLUKA starting from standard evaluated databases (mostly ENDF/B-VII, JENDL and JEFF).

Transport in arbitrarily complex geometries, including magnetic fields, can be accomplished using the FLUKA combinatorial geometry. A suitable voxel geometry module allows modelling properly CT scans or other detailed 3D representations of humans, typically for dosimetry or therapy planning purposes.

The code has the ability to run either in fully analogue mode, or in biased mode exploiting a rich variety of variance reduction techniques.

FLUKA is jointly developed by the European Laboratory for Particle Physics (CERN), and the Italian National Institute for Nuclear Physics (INFN) in the framework of an international collaboration. The approach to hadronic interaction modelling adopted in FLUKA has been described in several papers [3,4]. In short, hadron-nucleon inelastic collisions are described in terms of resonance production and decay up to a few GeV.

At higher energies, a model based on the Dual Parton Model [5] (DPM) takes over. Hadron-nucleus ( $h - A$ ) interactions as modelled in FLUKA can be schematically described as a sequence of the following steps:

- Glauber-Gribov cascade and its high energy collisions;
- (Generalised)-intranuclear cascade;
- pre-equilibrium emission;
- evaporation/fragmentation/fission and final de-excitation.

Some of the steps can be omitted by design depending on the projectile energy and identity. Nucleus-nucleus collisions are treated by three different models depending on the energy range; details about the nuclear models can be found in [6] and references therein.

The simulation of the electromagnetic cascade in FLUKA is very accurate, including the Landau-Pomeranchuk-Migdal effect and a special treatment of the tip of the bremsstrahlung spectrum. Electron pairs and bremsstrahlung are sampled from the proper double differential energy-angular distributions improving the common practice of using average angles. In a similar way, the three-dimensional shape of the electromagnetic cascades is reproduced in detail by a rigorous sampling of correlated energy and angles in decay, scattering, and multiple Coulomb scattering. Tabulations for pair production, photoelectric and total coherent cross-sections as well as for atomic form factor data are based on the EPDL97 [7] photon cross-section library.

Bremsstrahlung, direct pair production and muon photo-nuclear interactions by muons are modelled according to state-of-the-art theoretical description and have been checked against experimental data.

Transport of charged particles is performed through an original Multiple Coulomb scattering algorithm [8], supplemented by an optional single scattering method.

Multiple scattering, taking into account nuclear form factors, is applied also to heavy ion transport. Up-to-date effective charge parametrisations have been employed, and straggling of ion energy loss is described in “normal” first Born approximation with the inclusion of charge exchange effects.

## **LHC and future high-energy projects**

LHC successfully ran up to 8 TeV cms with record luminosity, providing, as a by-product, plenty of data of relevance for machine protection, shielding, and other applications.

Comparisons with p-p (and Lead-Lead) event generators have shown areas where improvements are required, with the exception of EMD results for Pb-Pb interactions, where predictions are remarkably accurate.

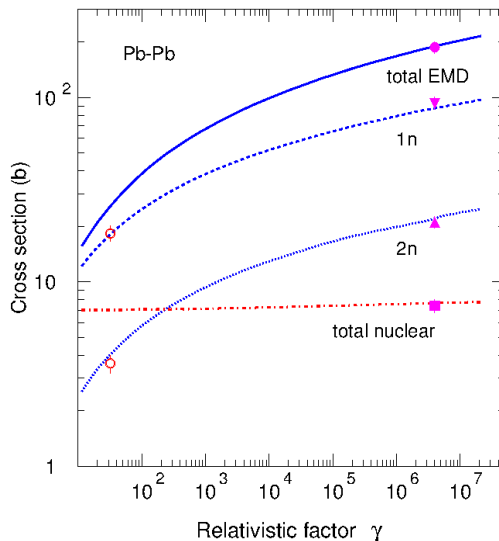
Model improvements are becoming critical, for the new LHC run at 7+7 TeV, where quenching margins will be much lower, for the forthcoming High Luminosity LHC upgrade (HL-LHC), and for the (hypothetical) Future Circular Collider, a 100 km ring hosting a proton-proton (50+50 TeV) collider and an electron-positron (up to 175+175 GeV) one.

## **Electro Magnetic Dissociation (EMD)**

The beam loss and collimation efficiency estimates at the LHC depend directly on predictions of the yields of fragments close in mass and charge to the initial ions. The distribution of magnetic rigidity (about 1%) of the fragments results in their being selectively lost in different places along the machine. One or both colliding nuclei can break-up in the high-intensity electromagnetic fields involved in ultraperipheral collisions without direct overlap of nuclear densities. At relativistic energies the Lorentz

contracted Coulomb fields of colliding nuclei can be represented as swarms of virtual photons. Absorption of equivalent photons by a nucleus leads to its excitation followed by various de-excitation processes via emission of neutrons, protons, mesons and even light nuclear fragments. Such photo-nuclear reactions are given the collective name electromagnetic dissociation of nuclei. FLUKA employs its internal nuclear interaction generator, PEANUT, in order to describe photo-nuclear reactions induced by both real and virtual photons. Electromagnetic dissociation has been implemented in this framework [9]. Comparisons of the results of simulations with data give very satisfactory results. As an example, Figure 1 shows the inclusive single and double neutron emission from 30 GeV/n to  $\sqrt{s}=2.76$  TeV/n. Nuclear fragmentation and electromagnetic dissociation of ions which occur in the LHC collimation system produce fragments close in mass and charge to beam ions. The fragments have similar magnetic rigidity and, therefore, remain close to the beam trajectory in the LHC ring for a long distance from the interaction point. This is primarily true for fragments created in electromagnetic dissociation of beam ions, as shown in Figure 2.

**Figure 1. Electromagnetic dissociation and nuclear cross-sections for Pb-Pb collisions as a function of the effective relativistic  $\gamma$  factor**



The results of calculations of the total EMD cross-section and partial cross-sections in 1n and 2n channels are shown by solid, dashed and dotted lines, respectively. Total nuclear cross-section calculated in the DPMJET-III [13] model is shown by dot-dashed line. Results from the ALICE collaboration [10] for the total EMD and nuclear cross-sections are shown by the full circle and full box, respectively. The measurements for 1n and 2n channels are shown by open circles [11] and full triangles [10].

### Improvements to Phojet/Dpmjet

For heavy ion interactions above 5 GeV/n, as well as for hadron-hadron and hadron-nucleus interactions above 20 TeV FLUKA interfaces to DPMJET-III [13], the nuclear framework around the PHOJET [16,17] event generator for hadron-hadron, photon-hadron and photon-photon collisions. Comparisons with LHC  $pp$  data at  $\sqrt{s}=7$  TeV showed discrepancies in the description of charged particle multiplicities. A satisfactory data agreement could be achieved by using an improved treatment of multiple parton interactions and fragmentation. Further developments are on-going, in particular regarding elastic scattering, where an approach based on the JLL model [14] has been selected. The dip-bump structure is generated through interference of terms associated with a two-component Pomeron, 2 effective Reggeons and an Odderon contribution. The model can be expressed in a simple analytic form, thus allowing for efficient MC sampling. The small number of free parameters ensures that extrapolations up to very

high energies stay reasonable. Once tuned to experimental data sets this model provides very good results from as low as  $\sqrt{s}=15$  GeV up to  $\sqrt{s}=7$  TeV, corresponding to a laboratory momentum as high as  $2.6 \cdot 10^4$  TeV/c. Using a single set of parameters, the preliminary model reproduces the available measurements from the ISR to the latest data from the TOTEM experiment [18,19] at the LHC, as shown in Figure 3.

**Figure 2. Cross-sections for the production of the heaviest fragments in electromagnetic dissociation of 2750 GeV/n Pb nuclei on  $^{12}\text{C}$  target as a function of the momentum-to-charge ratio normalised to that of the main circulating beam**

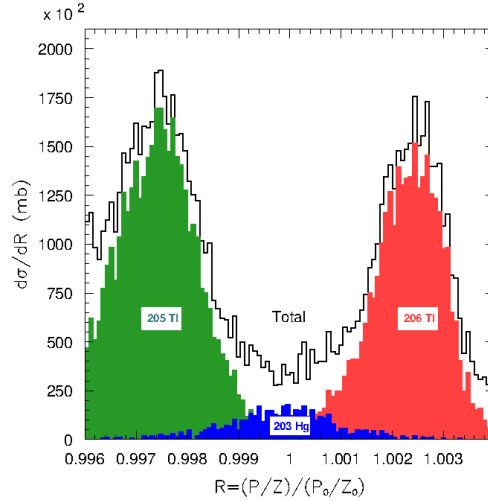
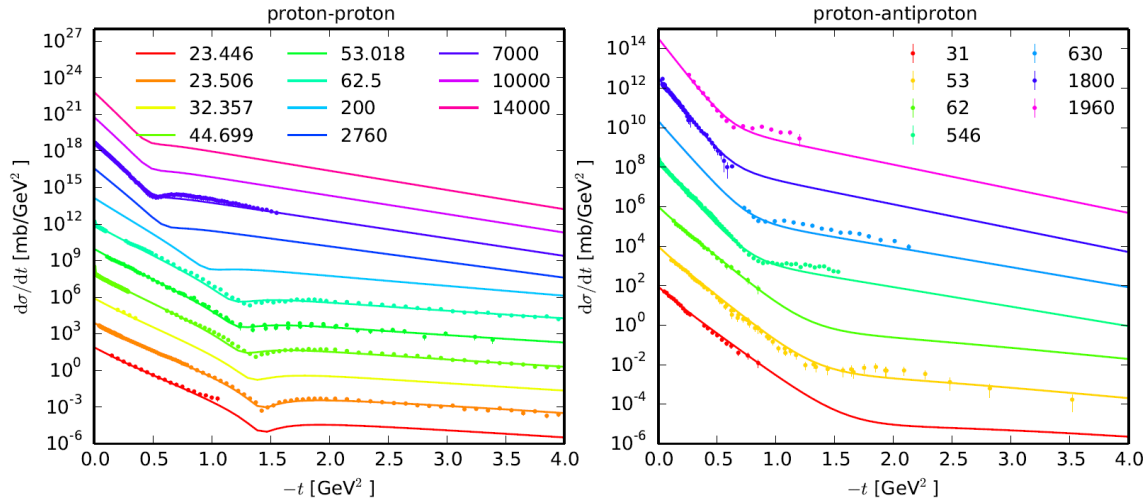


**Figure 3. Elastic cross-section for proton-proton and proton-antiproton scattering at different centre of mass energies [GeV]**



Lines are simulated results and points are experimental data [15]. Energy sets are multiplied by an increasing power of ten.

### Synchrotron radiation

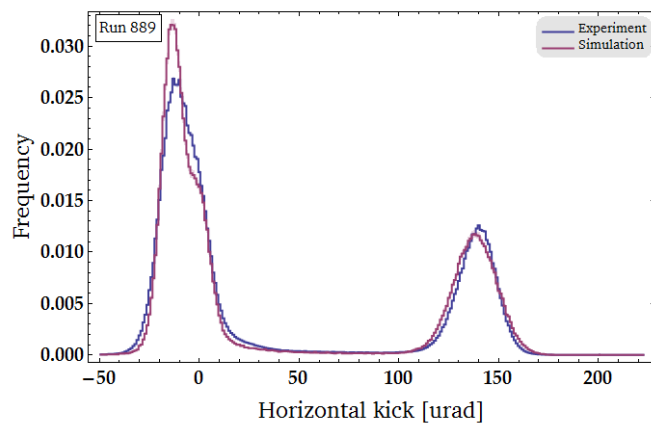
Synchrotron radiation is a limiting issue for possible future high energy  $e^+e^-$  circular colliders, like the proposed FCCee at CERN. The ability to easily compute synchrotron radiation emission is an obvious advantage for these studies, as well as for all calculations related to synchrotron radiation sources.

Sophisticated low-energy photon transport including polarisation effects and full account for bound electron effects has been available in FLUKA for several years [20]. Recently, a new dedicated source for SR radiation has been added to the collection of ready-to-use options in FLUKA. It includes sampling from the appropriate photon spectrum, polarisation as a function of the emitted photon energy, proper angular distribution. Arbitrary orientation of the emitting particles with respect to an external magnetic field can be treated, as well as the emission along accelerator arcs and helical paths.

### Crystal channeling

Charged particles entering a crystal close to some preferred direction can be trapped in the electromagnetic potential well existing between consecutive planes or strings of atoms. This channeling effect can be used to extract beam particles if the crystal is bent beforehand. Crystal channeling is becoming a reliable and efficient technique for collimating beams and removing halo particles. At CERN, the installation of silicon crystals in the LHC is under scrutiny by the UA9 [21] collaboration with the goal of investigating if they are a viable option for the collimation system upgrade.

**Figure 4. Distribution of angular deflections given by a strip crystal to 400 GeV protons**



Results from the simulation, using FLUKA model for channeling, are shown in red and compared to the UA9-H8 [24] experiment conducted at CERN, in blue.

A new Monte Carlo model of planar channeling has been developed from scratch [22] in order to be implemented in the FLUKA code. Crystal channels are described through the concept of continuous potential taking into account thermal motion of the lattice atoms and using Molière screening function. The energy of the particle transverse motion determines whether or not it is trapped between the crystal planes while single Coulomb scattering on lattice atoms can lead to dechanneling. Volume capture and reflection applying to quasi-channeled particles are also modelled. Similarly to dechanneling, single scattering is used to determine the occurrence of volume capture. The parameters of the crystals, such as torsion or miscut, are described as well. Work is on-going on the implementation of a reduced energy loss for channeled particles. This model has been successfully benchmarked [22] against data taken by the UA9-H8 experiment with a 400 GeV/c proton beam. An example of the results is shown in Figure 4, where the

experimental distribution of deflected protons downstream the crystal compares nicely to the simulation.

### Spin and parity effects

All nuclear interaction models, including those generated by ions, share parts of the common PEANUT framework. In particular, all nuclear fragments, irrespective of the originating reaction, are de-excited through the same evaporation/fragmentation and gamma production chain. The final steps of the reaction include evaporation in competition with fission and gamma de-excitation.

The FLUKA evaporation model, which is based on the Weisskopf-Ewing approach, has been continuously updated over the years, with the inclusion, for instance, of sub-barrier emission, full level density formula, analytic solution of the emission widths, evaporation of nuclear fragments up to  $A \leq 24$ . As a result, the code can be reliably used for the prediction of induced radioactivity and residual dose in most of the cases of interest for radioprotection. However, spin/parity dependent evaporation (Hauser-Feshbach) is still too complex to be implemented in MC codes in the energy range of interest for FLUKA applications. Furthermore, it is difficult to keep track of the total angular momentum and parity evolution of the system during the cascade and pre-equilibrium stages, particularly at medium/high energies. As a consequence, isomer production with respect to ground state production cannot be reliably computed. Similarly, individual level population and the subsequent gamma emission are hard to predict.

The first attempts to enforce spin/parity conservation in PEANUT targeted the Fermi break-up part in cases when initial conditions are well defined. Statistical evaporation of excited low mass fragments is unsuitable due to the relatively few, widely spaced levels. Therefore, alternative de-excitation mechanisms are employed for these light (typically  $A \leq 16$ ) residual nuclei in most Monte Carlo (MC) codes. A popular choice for this calculations is the Fermi Break-up model [25,26], where the excited nucleus is supposed to disassemble in one single step into two or more fragments, possibly in excited states, with branching given by plain phase space considerations.

However, the basic formulation of Fermi Break-up implicitly assumes that the fragment emission occurs in  $L=0$  and neglects whichever consideration of the initial spin and parity state,  $J^\pi$ , of the excited nucleus. If the initial  $J^\pi$  is known, suitable modifications must be applied in order to account for it, in particular:

- The minimum orbital momentum  $L_{min}$  compatible with  $J^\pi$  and the spins and parities of the emitted particles must be computed.
- The spin factor  $S_n$  must be restricted to the spin projections compatible with an emission with  $L_{min}$ .
- In case  $L_{min} > 0$ , a suitable centrifugal barrier must be added to  $E_{Coul}$ .

Figure 5 shows the example of the improvement due to the inclusion of spin/parity considerations, where the calculated excitation curve for  $^{12}\text{C}(\gamma, n)^{11}\text{C}$ , a reaction for which  $J^\pi = 0^+$  in the GDR energy range, is compared with experimental data before and after their application. This reaction is of special relevance for underground experiments, particularly those using liquid scintillators, where photons produced by high-energy muons penetrating through the underground rock can produce  $^{11}\text{C}$  and neutrons which represent a background.

Recently, work has started also for standard evaporation at low excitations, together with the implementation of the MLO (Modified Lorentzian) model for the competition between particle evaporation and  $\gamma$  emission. As an example, Figure 6 shows good agreement in the prediction of the excitation function for double neutron emission after

photon absorption on gold. A perfect application for this new treatment is the EMD process described beforehand, because the initial state after the virtual photon absorption has definite spin and parity.

### Developments of interest for hadrontherapy monitoring

FLUKA is routinely used at the CNAO and HIT hadron therapy centres for the generation of Treatment Planning System (TPS) databases and for TPS verification. It is also used as a research tool, for instance for the investigation of new beams and new methods for therapy monitoring. The latter research field is also the scope of the ENVISION/ENTERVISION European programmes.  $^{16}\text{O}(\text{p}, \text{x})^{15}\text{O}$  and  $^{12}\text{C}(\text{p}, \text{x})^{11}\text{C}$  are the most important reactions for in-vivo or off-line PET (Positron Emission Tomography) monitoring of proton therapy [27]. These reactions can proceed through the emission of either independent nucleons or deuterons. A reliable prediction of these channels, particularly at energies typical of the Bragg peak region for protons, is critical. Composite ejectiles like d, t,  $^{3}\text{He}$ , and  $\alpha$  can be reasonably described by coalescence algorithms during the IntraNuclear Cascade and pre-equilibrium stages. All possible combinations of unbound nucleons and/or light fragments are checked at each stage of system evolution and a figure-of-merit evaluation based on phase space “closeness” at the nucleus periphery is used to decide whether a light fragment is formed rather than not. This approach works reasonably well at medium/high energies: It has been recently extended up to Intermediate Mass Fragments of mass  $A \leq 10$  [28]. However, at energies below a few tens of MeV, coalescence is increasingly ineffective in reproducing experimental data. Recently, a direct deuteron formation mechanism following the first  $pn$  or  $np$  elementary interaction has been implemented in FLUKA which greatly improved the predictive power for reactions like  $(\text{p}, \text{d})$ . Examples outlining the effectiveness of the new approach can be found in [30]. Another promising technique for in-vivo hadrontherapy monitoring relies on the detection of prompt photons emitted following nuclear interactions by the beam particles. FLUKA capabilities in this aspect have been recently enhanced, as described in [30,31].

**Figure 5.**  $^{12}\text{C}(\gamma, \text{n})^{11}\text{C}$  cross-sections as computed with FLUKA2013.0 (red, upper curve), and FLUKA2011.2 (blue curve) compared with data retrieved from the EXFOR [29] library

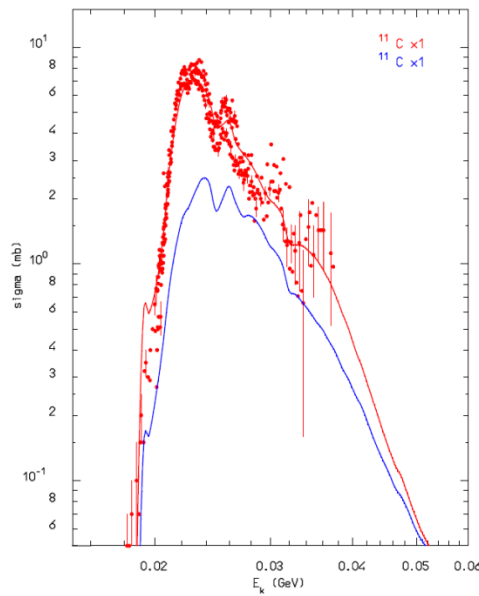
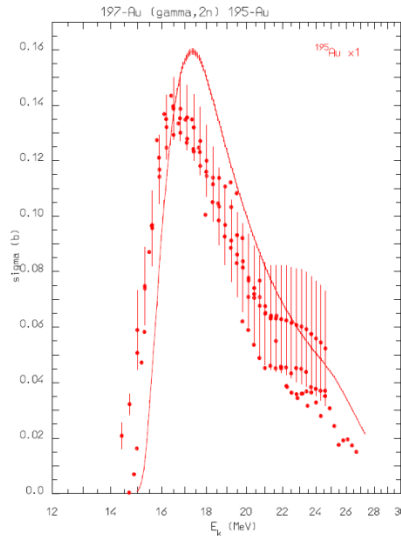


**Figure 6. Cross-section for the production of  $^{195}\text{Au}$  from photon absorption on  $^{197}\text{Au}$ , as a function of the incoming photon energy**



Dots: experimental data [29], line: FLUKA simulation.

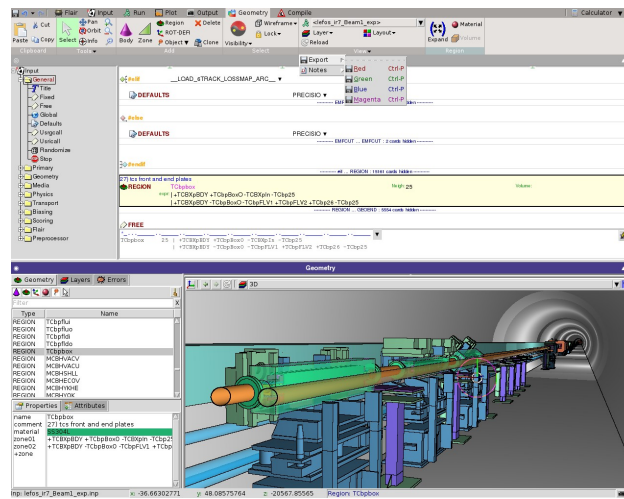
## Technical advancements

Besides its physics capabilities, FLUKA is also becoming an increasingly flexible and user-friendly tool.

### The LineBuilder

The FLUKA geometry allows for easy replication of basic structures, as well as rotations, translations and scaling of selected elements. These features were exploited to develop the “LineBuilder” (LB) tool, now essential for any LHC related simulation. The LineBuilder consists of a database of accelerator components and of an assembler of geometries. The actual beam lines are automatically generated through direct use of machine optics files, thus ensuring protection against wrong settings of the beam line, e.g. misplacements, wrong orientations, mismatches in magnetic fields and collimator apertures. An example of LB results, as visualised by Flair is shown in Figure 7.

**Figure 7. Example of beam line geometry generated with the LB package**



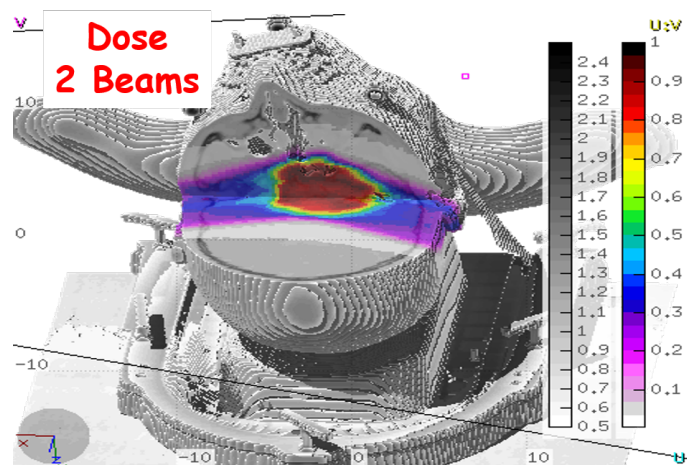
### Coupling with SixTrack

Machine protection is a multi-disciplinary field, based on radiation-matter interaction and particle dynamics in accelerators: Typical Monte Carlo results (energy deposition, particle fluence, signals in monitors...) are affected by multi-turn effects, namely particles that interact but stay within the accelerator acceptance and reappear in the same place after one or even more turns. On the other hand, particle scatterings in intercepting devices may cause beam losses far away from the interaction point. This interplay between Monte Carlo and accelerator transport is now accurately accounted for with the recent coupling [32] between FLUKA and SixTrack. SixTrack is a 6D transport code routinely used for single particle tracking in high energy circular machines (e.g. LHC and RHIC), especially for dynamic aperture and collimation studies. FLUKA and SixTrack run independently at the same time, communicating with each other. One or more portions of the accelerator lattice are covered by FLUKA, the rest by SixTrack. The two codes exchange particles at run-time through a network port, by means of a dedicated communication protocol (C/C++). The advantages of this coupling are more accurate predictions, relying on the best of the two codes, self-consistency, limited human intervention.

### Flair: graphical user interface

Flair [33] is a user-friendly graphical interface for FLUKA Monte Carlo transport code. It provides an Integrated Development Environment (IDE) for all stages of FLUKA simulations, from building an error-free input file, debugging, creation of user-written routines, execution, status monitoring, data processing and plot generation. Its use greatly enhances the productivity of users and provides a less steep learning curve for beginners. Flair includes real-time geometry visualisation and graphical editing, both with two-dimensional cross-section cuts and with three-dimensional projections. To facilitate the use of FLUKA for medical applications, Flair integrates intuitive PET scanner geometry generator and importing routines for processing DICOM [34] files. DICOM is a non-proprietary data interchange protocol used in medicine. 3D CT scans, MRI, PET dose maps, as well dose distribution from the treatment planning systems all use the DICOM format to exchange their information. Flair is able to import the DICOM files (see Figure 8) and convert them in FLUKA voxel geometries.

**Figure 8. Three-dimensional rendering of a CT scan converted by Flair into the FLUKA voxel geometry**



Simulated dose delivery with a two-beam proton treatment is superimposed to the geometry.

## Conclusions

The FLUKA code is used for a variety of applications at CERN and elsewhere. Some of the recent improvements have been described, together with examples showing the improved results when compared with experimental data.

## Acknowledgments

This research project was partially supported by ENVISION, which is co-funded by the European Commission under FP7 Grant Agreement N. 241851.

## References

- [1] A. Ferrari, P.R. Sala, A. Fassò, J. Ranft (2005), "FLUKA: a multi-particle transport code", CERN-2005-10, INFN/TC\_05/11, SLAC-R-773.
- [2] G. Battistoni et al. (2007), *AIP Conference Proceedings* 896, p. 31.
- [3] A. Ferrari, P.R. Sala (1998), "The Physics of High Energy Reactions", *Proceedings of Workshop on Nuclear Reaction Data and Nuclear Reactors Physics, Design and Safety*, A. Gandini, G. Reffo eds., Trieste, Italy, April 1996, 2, p.424.
- [4] G. Battistoni et al. (2006), *Proceedings of 11<sup>th</sup> International Conference on Nuclear Reaction Mechanisms*, Varenna, Italy, 12-16 June 2006, E. Gadioli ed., p. 483.
- [5] A. Capella, U. Sukhatme, C-I. Tan, J. Tran Thanh Van (1994), *Phys. Rep.* 236, p. 225.
- [6] F. Ballarini et al. (2007), *Adv. Space Rad.* 40, p. 1339.
- [7] D.E. Cullen et al. (1997), "EPDL97: The Evaluated Photon Data Library, '97 Version", UCRL- 50400, Vol. 6, Rev. 5.
- [8] A. Ferrari, P.R. Sala, R. Guaraldi, F. Padoani (1992), *Nucl. Instr. and Meth. B* 71, p. 412.
- [9] H.H. Braun et al. (2014), *Phys. Rev. ST Accel. Beams* 17, 021006.
- [10] B. Abelev et al. (2012), *Phys. Rev. Lett.* 109, 252302.
- [11] M. B. Golubeva (2005), *Phys. Rev. C* 71, 024905.
- [12] T. Sjöstrand, S. Mrenna and P. Skands (2006), *JHEP* 5 p. 26.
- [13] S. Roesler, R. Engel, J. Ranft (2001), "The Monte Carlo event generator DPMJET-III", *Proceedings of the MonteCarlo 2000 Conference*, Lisbon, October 23–26 2000, A. Kling, F. Barão, M. Nakagawa, L. Távora, P. Vaz eds., Springer-Verlag Berlin, p. 1033.
- [14] L.L. Jenkovszky et al. (2011), *Int. Jour. Mod. Phys. A* 26 p.4755.
- [15] J.R. Cudell: <http://www.theo.phys.ulg.ac.be/~cudell/data/>.
- [16] R. Engel (1995), *Z. Phys. C* 66, p. 203.
- [17] R. Engel, J. Ranft (1996), *Phys. Rev. D* 54, p. 4244.
- [18] "The TOTEM Collaboration" (2011), *EPL* 96, 21002.
- [19] "The TOTEM Collaboration" (2011), *EPL* 95, 41001.
- [20] T. T. Bohlen, A. Ferrari, V. Patera and P. R. Sala (2012), *JINST* 7) P07018.
- [21] <http://home.web.cern.ch/about/experiments/ua9>.
- [22] P.J. Schoofs (2014), Monte Carlo Modeling of Crystal Channeling at High Energies, These Ecole polytechnique federale de Lausanne EPFL, nr. 6046.

---

- [23] P. Schoofs, F. Cerutti, A. Ferrari, G. Smirnov (2013), *Nucl. Instr. and Meth. in Phys. Res. B*, 309, p. 115.
- [24] M. Pesaresi et al. (2011), *JINST* 6 P04006.
- [25] E. Fermi (1950), *Prog. Theor. Phys.* 5, p. 1570.
- [26] M. Epherre and, E. Gradsztajn (1967), *J. Phys.* 28, p. 745.
- [27] K. Parodi, A. Ferrari, F. Sommerer, H. Paganetti (2007), *Phys. Med. Biol.* 52 p. 3369.
- [28] A. Boudard et al. (2013), *Phys. Rev.* C87, 014606.
- [29] <http://www-nds.iaea.org/exfor/>.
- [30] A. Ferrari et al. (2013), “The FLUKA Code: Developments and Challenges for High Energy and Medical Applications”, Proc. of ND2013, in press.
- [31] G. Battistoni et al. “Modeling prompt photon emission with FLUKA”.
- [32] A. Mereghetti et al. (2013), “SixTrack-Fluka active coupling for the upgrade of the SPS scrapers”, *Proceedings of IPAC2013*, Shanghai, China, 2013.
- [33] V. Vlachoudis (2009), *Proc. of Int. Conf. on Math, Comp Meth & Reactor Physics*, Saratoga Springs, NY, <http://www.fluka.org/flair>.
- [34] National Electrical Manufacturers Association (1996), NEMA Standard Publications PS 3.